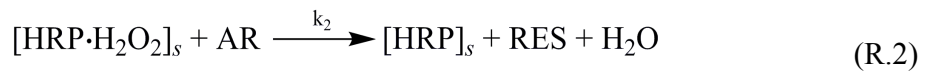
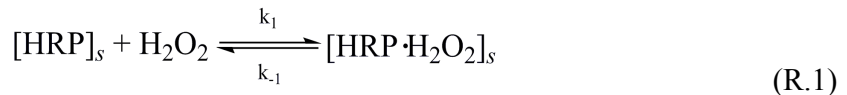


Supplemental Information

I. Derivation of the Modified Eley-Rideal Mechanism

As a convention bracket symbols are used to represent concentration (or activity in the limit of unit activity coefficient), while subscript “*s*” indicates a species adsorbed on the surface. Horseradish peroxidase, amplex red, and resorufin are abbreviated HRP, AR, and Res, respectively. The proposed reaction mechanism is as follows. Surface immobilized horseradish peroxidase $[HRP]_s$ reacts with H_2O_2 forming an $[HRP \cdot H_2O_2]_s$ complex (R.1). This complex then irreversibly reacts with AR to produce $[HRP]_s$, Res, and H_2O (R.2).



The rates of formation of resorufin and of the intermediate are given below:

$$r = \frac{d[Res]}{dt} = k_2 [HRP \cdot H_2O_2]_s [AR] \quad (S1)$$

$$\frac{d[HRP \cdot H_2O_2]_s}{dt} = k_1 [HRP]_s [H_2O_2] - k_{-1} [HRP \cdot H_2O_2]_s - k_2 [HRP \cdot H_2O_2]_s [AR] \quad (S2)$$

A site balance yields the concentration of free HRP sites in terms of the total HRP on the surface and the intermediate:

$$[HRP]_s = [HRP_T]_s - [HRP \cdot H_2O_2]_s \quad (S3)$$

Applying the pseudo-steady state hypothesis to the intermediate, we set Eq. (2) equal to zero, substitute Eq. (3) into Eq. (2), and solve for the $[HRP \cdot H_2O_2]_s$ complex:

$$[HRP \cdot H_2O_2]_s = \frac{k_1 [HRP_T]_s [H_2O_2]}{k_1 [H_2O_2] + k_2 [AR] + k_{-1}} \quad (S4)$$

Substituting Eq. (4) into Eq. (1) yields the overall rate equation:

$$r = \frac{k_1 k_2 [HRP_T]_s [AR] [H_2O_2]}{k_1 [H_2O_2] + k_2 [AR] + k_{-1}} \quad (S5)$$

Case 1: Planar surface reaction with H_2O_2 in excess:

When the concentration of H_2O_2 is large, it is essentially constant. This case is frequently realized, for example in the experiments discussed in the text in which the $[H_2O_2]$

$= 2mM$, which is at least 5 times greater than the initial concentration of AR. Therefore we can rearrange Eq. (5) into a Michaelis-Menten like expression in terms of AR:

$$r = k_1 [\text{HRP}_T]_s [\text{H}_2\text{O}_2] \frac{[\text{AR}]}{\frac{k_1 [\text{H}_2\text{O}_2] + k_{-1}}{k_2} + [\text{AR}]} = V'_m \frac{[\text{AR}]}{K'_m + [\text{AR}]} \quad (\text{S6})$$

where V'_m and K'_m are the maximum rate and Michaelis-Menten constant with respect to AR, respectively.

$$V'_m = k_1 [\text{HRP}_T]_s [\text{H}_2\text{O}_2] \quad (\text{S7})$$

$$K'_m = \frac{k_1 [\text{H}_2\text{O}_2] + k_{-1}}{k_2} \quad (\text{S8})$$

Case 2: Planar surface reaction with Amplex Red in excess:

We make a similar assumption as in Case 1, and get a Michaelis-Menten like rate equation in terms of H_2O_2 .

$$r = k_2 [\text{HRP}_T]_s [\text{AR}] \frac{[\text{H}_2\text{O}_2]}{\frac{k_2 [\text{AR}] + k_{-1}}{k_1} + [\text{H}_2\text{O}_2]} = V''_m \frac{[\text{H}_2\text{O}_2]}{K''_m + [\text{H}_2\text{O}_2]} \quad (\text{S9})$$

Where V''_m and K''_m are the maximum rate and Michaelis-Menten constant with respect to H_2O_2 , respectively.

$$V''_m = k_2 [\text{HRP}_T]_s [\text{AR}] \quad (\text{S10})$$

$$K''_m = \frac{k_2 [\text{AR}] + k_{-1}}{k_1} \quad (\text{S11})$$

Case 3: Nanopore reaction

In the case of the nanopore experiments, both $[\text{AR}]$ and $[\text{H}_2\text{O}_2]$ are small. However, it would be impractical to run kinetic simulations on all parameters given in the overall rate equation in Eq. (5), so we seek a more convenient form using scaling arguments. Since the initial concentrations of H_2O_2 and AR are similar, we use the same scaling, C_o , for both:

$$[\text{H}_2\text{O}_2]^* = \frac{[\text{H}_2\text{O}_2]}{C_o} \quad (\text{S12})$$

$$[\text{AR}]^* = \frac{[\text{AR}]}{C_o} \quad (\text{S13})$$

$$r^* = \frac{r \cdot k_{-1}}{k_1 k_2 [HRP_T]_s C_o^2} \quad (S14)$$

where * indicates a nondimensional quantity of order 1. Making these substitutions, we get the following rate expression:

$$r^* = \frac{[AR]^* [H_2O_2]^*}{\frac{k_1}{k_{-1}} C_o [H_2O_2]^* + \frac{k_2}{k_{-1}} C_o [AR]^* + 1} \quad (S15)$$

We assume that since $C_o \ll 1$, and since $(k_1/k_{-1})(k_2/k_{-1})$, $[H_2O_2]^*$, and $[AR]^*$ are all ≈ 1 , then the first two terms in the denominator of Eq. (15) can be neglected, *i.e.*

$$\frac{k_1}{k_{-1}} C_o [H_2O_2]^* \ll 1 \quad (S16)$$

$$\frac{k_2}{k_{-1}} C_o [AR]^* \ll 1 \quad (S17)$$

These assumptions reduce the rate equation to a simple bimolecular form which is shown below in nondimensional, dimensional, and simplified dimensional form:

$$r^* = [H_2O_2]^* [AR]^* \quad (S18)$$

$$r = \frac{k_1 k_2 [HRP_T]_s}{k_{-1}} [H_2O_2] [AR] \quad (S19)$$

$$r = k_T [H_2O_2] [AR] \quad (S20)$$

Eq. (20) gives the final form of the rate equation used in our simulations. We emphasize that this form holds only when both substrates are present at low concentration.

II. Concentration Approximations

Homogeneous solution experiments:

The enzyme concentration in reference (9) is 0.01 u/mL, which at an activity of 250 u/mg and assuming a molecular weight of 44 kDa for HRP, yields a concentration of $\sim 1 \times 10^{-3}$ μM . Other values (enzyme molecules consumed, K_m , V_m) were taken directly from the reference, and we calculate an initial rate of $1.8 \mu\text{M min}^{-1}$ using the Michaelis-Menten equation, assuming $[H_2O_2] = 50 \mu\text{M}$.

Planar surface experiments:

We calculate the maximum possible coverage of adsorbed HRP, from the area of the reaction zone (5 mm long x 100 μm wide) divided by the hydrodynamic cross sectional area

of HRP ($3 \times 3 \text{ nm}$) to get $\sim 10^{10}$ molecules of HRP on the microchannel surface. It is likely the actual surface coverage is much less, but this provides a maximum bound for comparison to the free solution experiment. We assign an analog of concentration of HRP in the planar surface experiments by taking the maximum number of HRP molecules which can adsorb to the surface divided by the volume contained in the microfluidic region ($5 \text{ mm long} \times 100 \mu\text{m wide} \times 50 \mu\text{m deep}$). The initial rates calculated from the experimental fits are shown in Fig. 6, assuming $[\text{AR}] = 50 \mu\text{M}$ and $[\text{H}_2\text{O}_2] = 50 \mu\text{M}$ for AR and H_2O_2 dependences, respectively.

NCAM experiments:

Similar to the planar surface experiments, we define the maximum possible HRP coverage by dividing the internal surface area of a single nanopore ($2\pi rh = 2\pi \times 200 \text{ nm} \times 10 \mu\text{m}$) by the hydrodynamic cross sectional area of HRP ($3 \times 3 \text{ nm}$), yielding $\sim 10^6$ HRP molecules per pore, and multiplying by ~ 1000 nanopores in the $400 \times 400 \mu\text{m}$ reaction area. This yields a maximum of 10^9 HRP molecules present, although the actual number of HRP molecules is likely much smaller. The “concentration” of HRP in the nanopore is calculated in a similar way, dividing the number of HRP molecules per pore by the pore volume ($\pi r^2 h = \pi \times 200^2 \text{ nm}^2 \times 10 \mu\text{m} \approx 10^{-15} \text{ L}$). This yields an exceptionally high HRP “concentration” of 10^{-3} M in the femtoliter sized reaction volume – a direct reflection of the enhanced surface-to-volume ratio characteristic of nanopores.

III. Working curve for Resorufin concentration

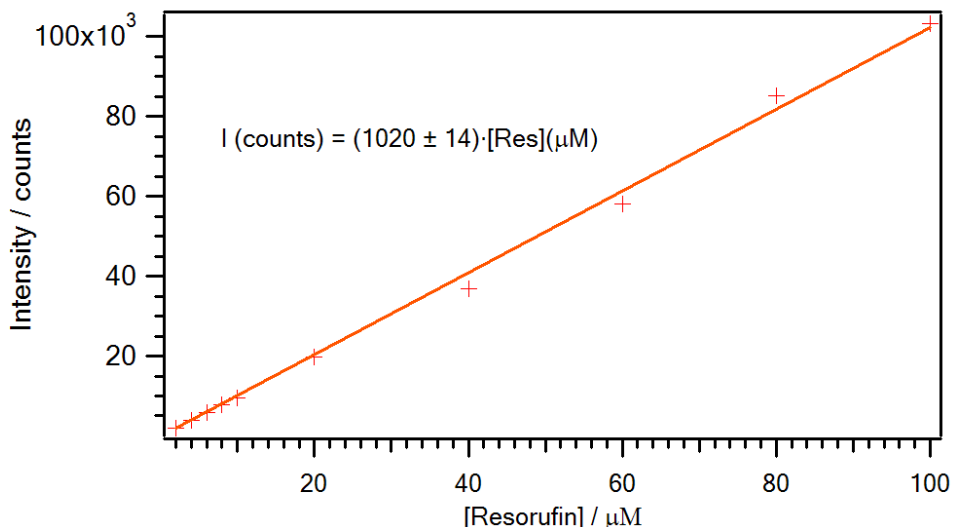


Figure S1. Working curve for intensity vs. concentration of resorufin. The red line is a linear fit with 0 as the intercept, equation shown. This working curve was used to analyze the data on planar surface.

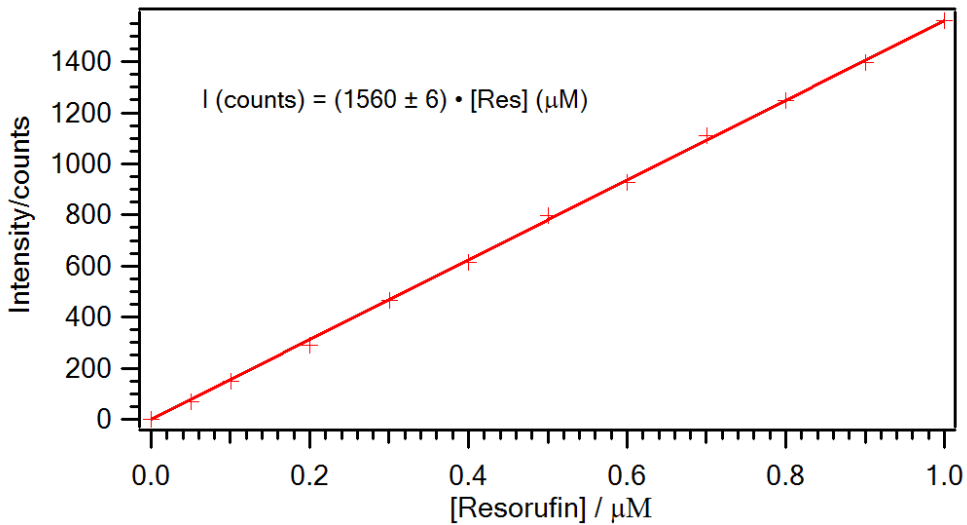


Figure S2. Working curve for intensity vs. concentration of resorufin. The red line is a linear fit with 0 as the intercept, equation shown. This working curve was used to analyze the data in NCAM experiments.

IV. Constants Used in Finite Element Simulation

The transport coefficients used in the finite element simulation are listed below. The diffusion coefficient applies to all reactant and product species (AR, RES, and H_2O_2). The electrophoretic mobilities of AR and RES were estimated to be similar to that of fluorescein, but the simulation result is not very sensitive to these values because fluid transport across the pore is mediated primarily by electroosmosis generated in the PDMS microchannel regions. The electroosmotic mobilities are defined as the Smulochowski slip velocity divided by the electric field strength. Since the nanopores are etched in polycarbonate, which generally has a weak surface charge density, the electroosmotic mobility for those boundaries was set to zero. Lastly, since the simulation geometry had only a single nanopore rather than an array of $\sim 10^3$ nanopores like in the experiment, the conductivity of the nanopore was set 10^3 times higher than that of the microchannel regions. This was necessary to approximately match the electric field strength in the nanopore to the experimental situation.

$$D = 10^{-9} \text{ m}^2\text{s}^{-1}$$

$$\mu_{\text{eof}} (\text{PDMS boundaries}) = 7 \times 10^{-8} \text{ m}^2\text{V}^{-1}\text{s}^{-1}$$

$$\mu_{\text{eof}} (\text{Nanopore boundaries}) = 0 \text{ m}^2\text{V}^{-1}\text{s}^{-1}$$

$$\mu_{\text{ep}} (\text{AR}) = -3 \times 10^{-8} \text{ m}^2\text{V}^{-1}\text{s}^{-1}$$

$$\mu_{\text{ep}} (\text{RES}) = -3 \times 10^{-8} \text{ m}^2\text{V}^{-1}\text{s}^{-1}$$

$$\mu_{\text{ep}} (\text{H}_2\text{O}_2) = 0 \text{ m}^2\text{V}^{-1}\text{s}^{-1}$$

$$\sigma (\text{Microchannels}) = 5.5 \times 10^{-6} \text{ Sm}^{-1}$$

$$\sigma (\text{Nanopore}) = 5.5 \times 10^{-3} \text{ Sm}^{-1}$$

V. Infrared Spectra of Polymers

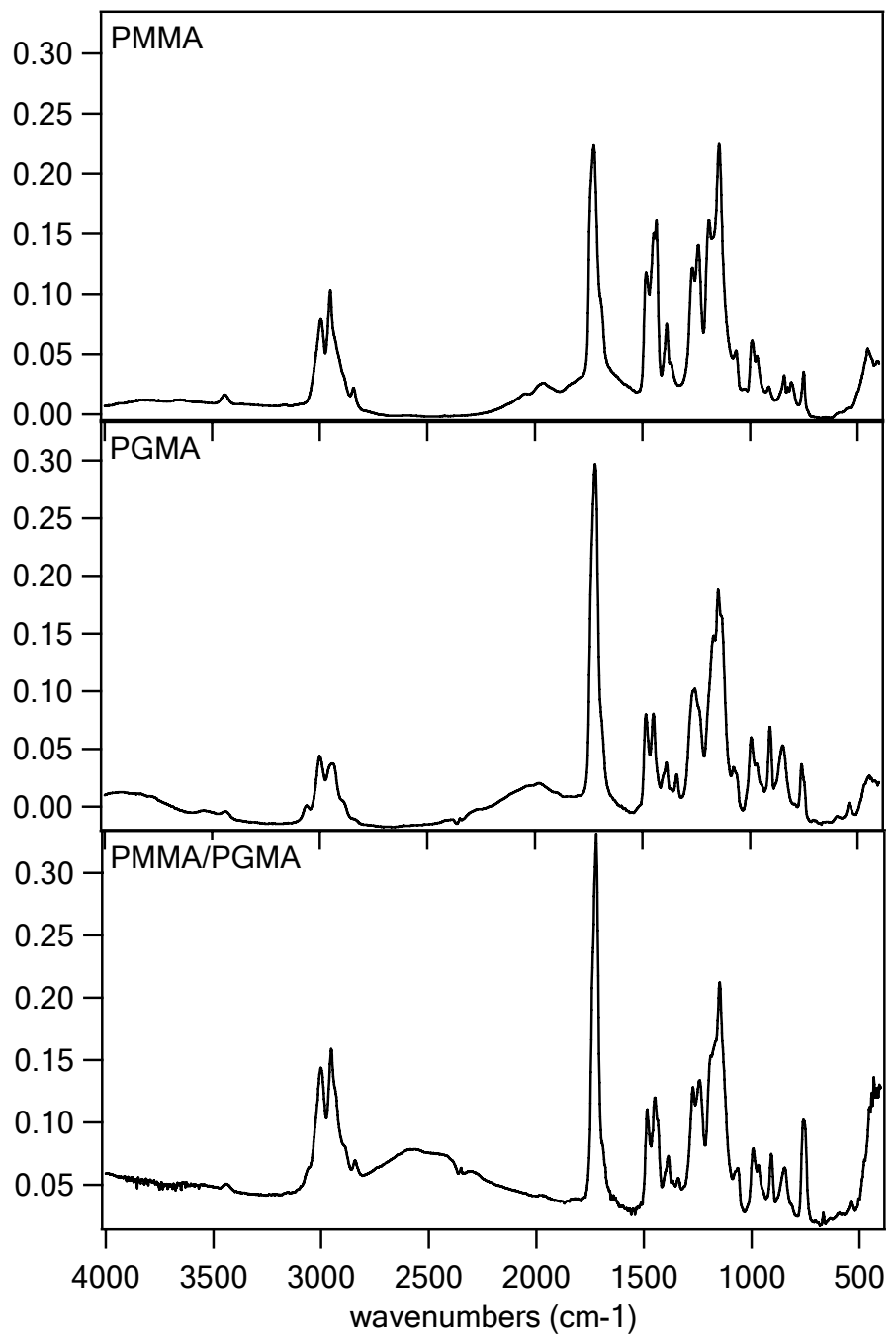


Figure S3. FTIR spectra for PMMA (*top*), PGMA (*middle*) and P(MMA-*co*-GMA) (*bottom*). The peaks at 845 cm⁻¹ and 905 cm⁻¹ are assigned to epoxy stretching.